Docampo P, Hanusch FC, Stranks SD, Doblinger M, Feckl JM, Ehrensperger M, Minar NK, Johnston MB, Snaith HJ, Bein T.

Solution Deposition-Conversion for Planar Heterojunction Mixed Halide Perovskite Solar Cells.

***Advanced Energy Materials* 2014, 4(14), 1400355.**

WILEY-VCH

DOI: 10.1002/((please add manuscript number))
Article type: Communication

Solution Deposition-Conversion for Planar Heterojunction Mixed Halide Perovskite Solar Cells

*Pablo Docampo,[†] Fabian Hanusch,[†] Samuel D. Stranks, Markus Döblinger, Johann M. Feckl Michael B. Johnston, Henry J. Snaith, Thomas Bein**

Dr. P. Docampo, F. Hanusch, Dr. M. Döblinger, Dr. J.M. Feckl, Prof. T. Bein
Department of Chemistry and Center for NanoScience (CeNS), University of Munich (LMU)
Butenandtstr. 11
81377 Munich, Germany
Fax: (+49-89-2180-77622)
E-mail: bein@lmu.de

Dr. S. Stranks, Prof. M. Johnston, Prof. H. Snaith
Condensed Matter Physics
University of Oxford
Parks Road
OX1 3PU, Oxford, UK

Keywords: ((maximum five, not capitalized, plural, separated by commas, no full stop))

Alkylammonium metal trihalide perovskite absorbers such as $MAPbI_3$ (MA: methylammonium) have recently garnered a considerable amount of interest recently in the photovoltaics community. Devices fabricated from these materials achieve very high power conversion efficiencies, already superior to amorphous Si. Previously reported record-breaking devices incorporate a solution processed planar heterojunction architecture based on the conversion of a planar PbI_2 layer into the $MAPbI_3$ perovskite. While high, the short circuit currents found in these devices are limited due to the short diffusion length of the neat $MAPbI_3$ perovskite. Here, we adapt the fabrication protocol to include chloride via the controlled addition of methylammonium chloride to the conversion solution. The resulting devices exhibit photocurrents of over 22 $mAcm^{-2}$ under equivalent AM1.5 sunlight conditions, exhibiting a ~10% improvement with respect to previous approaches. We find that the presence of chloride critically influences the lifetime of the photoexcited species in the active material and reduces the

series resistance of the devices, thus enabling almost complete sunlight capture and conversion in very thin solid films.

Introduction

Alkylammonium metal trihalide perovskite absorbers first employed in working photovoltaic devices were based on liquid electrolyte sensitized solar cells. Introduced by Kojima *et al.*, they exhibited a starting point power conversion efficiency of 3.8% with further work quickly extending it to over 6%.[1] It wasn't until a solid-state configuration was employed, however, that high device efficiencies were achieved.[2] Initial results were reported at 9% for perovskite sensitized titania-based devices, [2b] and further improvements were simultaneously achieved in a "meso-superstructured" configuration by replacing the mesoporous TiO_2 scaffold with an electronically inactive mesoporous Al_2O_3 layer, exhibiting device efficiencies of over 12%.[2c, 3] Some of the key advantages for this material system over other competing device concepts are that they are compatible with solution-processing techniques and can be fully processed at low temperatures, enabling their use in flexible device applications.[4]

Recently, Burschka *et al.* have demonstrated a method whereby an initial PbI_2 film is deposited over a mesoporous TiO_2 structure, which is then fully converted into the methylammonium lead triiodide ($MAPbI_3$) perovskite via a second step.[5] The lead iodide coated substrates are immersed in a methylammonium iodide (MAI) solution in isopropanol for a short time (< 1min), resulting in the conversion of PbI_2 into the perovskite phase. The resulting films are coated with the hole transporter 2,2',7,7'-Tetrakis[N,N-di(4-methoxyphenyl)amino]-9,9'-spirobifluorene (Spiro-MeOTAD) and a metal cathode, resulting in solar cells which approach the 15% benchmark.[6] Recently, this fabrication method was extended for planar heterojunction based devices by Liu *et al.* where a planar PbI_2 film was deposited over a ZnO blocking layer, and was then converted into the $MAPbI_3$ perovskite in a

second step. [7] This resulted in perovskite crystal sizes ranging from 100 to 1000 nm and an average thickness of ~300 nm. The resulting device performance of 15.7% is currently the highest performance achieved for perovskite solar cells, pointing towards planar heterojunction devices as a promising device architecture for further technological improvements.

The short circuit currents demonstrated for the devices prepared by Liu and coworkers of 20.4 $mAcm^{-2}$,[7] while high, are still short of the maximum current of over 22 $mAcm^{-2}$ reasonably achievable, taking into account other light capture losses for this material.[3a] A crucial limitation in this respect is the low diffusion length of the photoexcited species in the $MAPbI_3$ perovskite of around ~100 nm.[8] This parameter can be greatly extended with the inclusion of chloride in the precursor solution to over 1 μm.[8a, 9] Furthermore, it has been recently shown that the inclusion of chloride is also beneficial for charge transport in the photoactive layer.[10] It is expected thus that the inclusion of chloride should result in improved short circuit currents and thus overall photovoltaic performance. It is worth noting here that for devices incorporating mesoporous TiO_2 photoanodes, the neat triiodide perovskite functions efficiently without the need for the extended diffusion length of the photoexcited species.[11] This is a result of the interpenetrated nature of the collection photoanode, which exhibits pore sizes in the order of tens of nanometers, which in effect reduces the distance electrons must travel to this magnitude before being collected. In the case of planar heterojunctions, electrons must travel the whole thickness of the film, which can sometimes exceed hundreds of nanometers and thus extended diffusion lengths are a requirement for efficient operation.

Here we present planar, fully solution-processed heterojunction solar cells based on the solution deposition-conversion technique. We highlight the criticality of chloride in MA lead halide perovskites via a controlled addition of methylammonium chloride (MACl) to the MAI

immersion solution. The resulting devices exhibited power conversion efficiencies approaching 15%, and more importantly, showed short circuit currents of over 22 $mAcm^{-2}$, representing a gain of over 10% over state-of-the-art devices.[7] The parameter most influenced by the presence of chloride is the photoluminescence lifetime of the photoexcited species in the device, which reaches values exceeding 300 ns, matching previously reported results for the solution processed mixed halide perovskite films.[8a] Additionally, a reduction of series resistance from 14 to 7 Ωcm^2 was also observed.

Results and Discussion

The solar cells developed in this work are composed of a TiO_2/Perovskite/Spiro-MeOTAD planar heterojunction, deposited on an FTO electrode and capped with a gold electrode (**Figure 1**). The perovskite deposition was performed in two steps: firstly, a ~200 nm PbI_2 film was deposited via spincoating, followed by full conversion into the $MAPbI_{3-x}Cl_x$ perovskite via immersion in a heated solution of a mixture of MAI and MACl in isopropanol (IPA). A cross section of the final device structure can be seen in **Figure 2e**. The initial PbI_2 film is shown in the cross sectional image in **Figure 2a-b**, where we can observe distinct PbI_2 sheets, oriented flat over the non-porous TiO_2 layer. The uniformity of the layer can be assessed from Figure 2b where we show an extended view of the cross section. Additionally, from the top views shown in **Figure 2c and 2d** we can see that the layer is smooth and covers 100% of the TiO_2-coated FTO glass substrate. After immersion, we can clearly observe the formation of the perovskite crystals, as shown in **Figure 2g**, with a mixture of crystal sizes ranging from approximately 100 to almost 600 nm in length. As can be seen in the low magnification image in **Figure 2h**, the surface coverage is approximately 100%.

To assess the impact of chloride addition on the structure, the films were analyzed via powder XRD after removal from the substrate. The perovskite films presented here are phase pure,

crystallized in the expected tetragonal I4/mcm space group.[12] No impurities were found, in contrast with other solution-deposition methods that usually exhibit a small fraction of crystalline PbI_2 and $MAPbCl_3$ (Figures S1-3).[2c, 13] However, the change of the lattice parameters, attributed to the presence of chloride, reported for perovskites formed within mesoporous scaffolds was not observed for the system presented here.[13] Moreover, samples of $MAPbI_{3-x}Cl_x$ perovskite prepared according to the established protocol in previous studies (spin-coating from a mixture of MAI/$PbCl_2$) also did not show a significant change of lattice parameters.[8a] A similar result was found for films grown within mesoporous Al_2O_3 templates (Figure S2). This suggests that the vast majority of the chloride ions present in the precursor solution are not incorporated in the final structure. The chloride content in the structure was under the detection limit of both EDX and EELS and could not be quantified (Figures S4-5). The photovoltaic performance of devices incorporating perovskite films fabricated with a range of MACl concentrations in the immersion solution is shown in **Figure 3**. We can clearly see major increases in all device parameters, particularly short circuit current and fill factor, even for low MACl concentrations. The maximum performance was obtained for concentrations of 5 wt% MACl, which resulted in a champion device exhibiting almost 15% power conversion efficiency, 22.8 $mAcm^{-2}$ short circuit current and an open circuit voltage approaching 1 V under 104 $mWcm^{-2}$ equivalent AM 1.5 sunlight. The average power conversion efficiency for the optimum fabrication protocol including MACl is 10.5%, which is much more efficient than the one found for neat triiodide of 5.5%. A histogram of device power conversion efficiencies is shown in the Supporting Information Figure S6 as well as an Incident Photon to Current Conversion Efficiency (IPCE) spectrum Figure S7. Once this peak MACl concentration is exceeded, the devices start exhibiting both lower short circuit currents and lower voltages. This is very likely due to the observed morphology changes of the films, which exhibit average crystal sizes exceeding those of the neat triiodide by approximately 50% (Figures S6-7), and the appearance of a larger number of gaps between the crystals.[8a]

Additionally, we quantified the series resistance present in the devices (see inset of Figure 3a) and observe a decrease from 14 ± 1 to 7 ± 1 Ωcm^2, upon addition of chloride. This clearly accounts for the improvement of the fill factor measured, and is consistent with previous observations of mixed halide perovskites.[10] The neat $MAPbI_3$ solar cells presented here perform significantly worse than state-of-the-art devices presented by Liu and coworkers.[7] This is very likely due to the larger grain size present in our films, as well as the use of a TiO_2 blocking layer, which increases series resistance and does not collect charge as efficiently at higher biases. However, the important parameter in terms of this work, short circuit current, is comparable between the two studies and thus represents a valid platform to compare neat and mixed halide perovskite solar cells.

The measured short circuit currents are consistent with those estimated from light absorption measurements inside an integrating sphere (Figure S10). We also find that increasing the MACl content in the immersion solution improves light absorption at the bandgap edge due to the marginally higher scattering of these films. However, there is little room for improvement in this regard for the devices prepared here, as only an extra ~5% photocurrent could be gained if 100% of the incoming light were to be absorbed. All the additional losses in overall light harvesting arise from parasitic absorption in the FTO and reflection at the glass/air and glass/FTO interfaces. If no losses were present in the system, a maximum short circuit current of 27.15 $mAcm^{-2}$ could be achieved. Both films fabricated from mixed halide or neat MAI absorb light similarly, however, neat MA lead triiodide films exhibit a 10% lower short circuit photocurrent.

In order to understand this difference, we have performed time-resolved photoluminescence measurements, shown in **Figure 4**, and the resulting decay parameters are summarized in **Table 1**. For the excitation intensity used, the PL is expected to arise mostly from recombination of free charges, as the exciton binding strength for this system is relatively low

(E_b ~ 40 meV).[14] For all samples measured, we observe clearly biexponential decay dynamics, which may be a result of the widely varying crystal sizes present in the films, ranging from very small crystals of around 100 nm to some that approach the micron scale. Neat MA lead triiodide films exhibit lifetimes for the fast component of approximately 18 ns and a slow component of ~55 ns (Table 1). We note that these decay dynamics are several factors slower than those measured previously for the same triiodide system deposited via spincoating,[8] even for the fast component measured in the devices presented in this work. Additionally, we note that previous measurements on the PL lifetimes for pure triiodide films were performed on films consisting of very small crystals in the range of tens to a hundred nanometers.[8] We can clearly see that the addition of chloride has a dramatic effect on the dynamics of the photogenerated species, where long lifetime values of over 300 ns were found for films immersed in a solution mixture exceeding 5 wt% of MACl, consistent with recent results for mixed halide perovskites.[8a] Increasing the concentration of MACl beyond this point does not result in longer lifetimes, consistent with previous calculations which predict that only a very small fraction of the chloride ions can in fact be incorporated in the structure.[13]

The differences in PL lifetime may account for the observed losses in short circuit photocurrent. Diffusion lengths could not be calculated for the presented films since the roughness of the perovskite film prevents a reasonable estimation using previously-employed techniques.[8, 15] However, as a first approximation we may use literature values for the diffusion coefficient (D_e) in MA lead triiodide films and scale the diffusion length (L_D) according to our measured PL lifetimes (τ) as $L_D = \sqrt{D_e \tau}$. In this way, we can roughly estimate a 200 nm diffusion length for neat triiodide films and over 800 nm for samples that have been treated with chloride. A diffusion length of 200 nm, while longer than estimated previously,[8b] is not sufficiently long for the films presented in this work, where a large fraction of the crystals clearly exceed this thickness (Figure S8). Moreover, to achieve close

to 100% charge collection, the diffusion length must approach 3 times the film thickness.[16] Thus, we can account for our photocurrent losses in samples that have not been prepared with chloride.

Conclusions

We have demonstrated that the short circuit current of solution-processed planar heterojunction solar cells can be improved via the addition of chloride in the immersion solution, overtaking those exhibited by current state-of-the-art devices. We have shown that planar PbI_2 films can be fully converted within 5 minutes to the $MAPbI_{3-x}Cl_x$ perovskite structure by immersion in a heated solution mixture of MAI and MACl. We find that the addition of chloride critically impacts the lifetime of photoexcited species in the active material, increases light absorption at the bandgap edge and reduces the device series resistance, enabling almost complete sunlight capture in 400 nm thick films. It is worth noting here that the diffusion length of photoexcited species of the neat triiodide perovskite prepared via the deposition-conversion technique is roughly 200 nm; longer than estimated for films deposited via other methods. For this reason, films prepared in this way perform well in comparison to previous reports of solution processed $MAPbI_3$ planar heterojunction devices.[8, 17] This indicates that the photovoltaic properties of the material are highly sensitive to the method of film formation and crystallization.

Experimental Section

Preparation of the Methylammonium salts: Methylammoniumiodide was prepared following a recipe published earlier.[2c] In short, 24 mL of methylamine solution (33 % in ethanol) was diluted with 100 mL of absolute ethanol. To this solution, a 10 mL aqueous solution of hydriodic acid (57 wt%) was added under constant stirring. After a reaction time of one hour

at room temperature, the solvents were removed by rotary evaporation. The obtained white solid was washed with dry diethyl ether and finally recrystallized from ethanol.

To prepare the hydrochloride salt of methylamine, the hydriodic acid solution was replaced by 15 mL of concentrated hydrochloric acid (37 % in water). The purification procedure was the same as described above.

Solar cell preparation: Fluorine doped tin oxide (FTO) coated glass sheets (7 Ω/□, Pilkington) were etched with zinc powder and HCl (2 M) to obtain the required electrode pattern. The sheets were then washed with soap (2% Hellmanex in water), de-ionized water, acetone, and methanol and finally treated under oxygen plasma for 5 minutes to remove the last traces of organic residues. The substrates were then coated with a sol-gel derived TiO_2 layer, prepared as previously described and calcined at 500 °C in air to achieve full anatase crystallization.[3a]

A 27.2 mM HCl solution in 2-propanol (Sigma Aldrich) (typical quantities of 2.53 mL of 2-propanol and 35 µL of 2 M HCl) was slowly added dropwise under vigorous stirring to a 0.43 M titanium isopropoxide solution in 2-propanol (typically 369 µL titanium isopropoxide in 2.53 mL of 2-propanol). The solution looked clear at all times, and was immediately discarded if cloudy.

A ~200 nm layer of lead iodide was deposited via spincoating from a 1 M PbI_2 solution in *N*,*N*-Dimethylformamide (DMF) at 3000 rpm for 15 s. To achieve optimum performance, it was critical to ensure that both the substrate and precursor solution temperature when starting the spincoater is between 60 and 65 °C. The spincoating was performed dynamically (i.e. the solution was added while the substrate was spinning) with a total 100 µL of solution, without allowing the substrates or solution to cool.

The stock immersion solutions were prepared by dissolving 10 mg/mL methylammonium iodide or methylammonium chloride in dry isopropanol, the latter with heating to 60 °C. For mixing the desired concentrations, these stock solutions were combined in the desired ratio.

Formatted: English (United States)

Before immersion, 40 mL of the solution and the PbI_2 films were heated to 60 °C on a hotplate. The temperature of the solution was monitored during the whole time with a thermometer. After immersion of the films into the solution in a square petri dish with the substrates face up, the solution was left undisturbed for 5 minutes. Once the conversion was finished, the films were washed with clean, anhydrous isopropanol and dried under a nitrogen stream.

After drying, the films were covered with a 400 nm layer of Spiro-OMeTAD (Borun Chemicals, 99.1% purity) "spiro". 96 mg of spiro were dissolved in 1 mL of chlorobenzene and mixed with 10 mL 4-*tert*-Butylpyridine (*t*BP) and 30 μL of a 170 $mgmL^{-1}$ bis(trifluoromethane)sulfonimide lithium salt (LiTFSI) solution in acetonitrile. This solution was spincoated at 1500 rpm for 45 seconds. Before evaporating the gold electrodes, Spiro-OMeTAD was allowed to oxidize in air over night at room temperature and 15-20% rel. humidity.

PL sample preparation: For the preparation of the PL samples glass slides were used instead of FTO substrates. The PbI_2 deposition and immersion procedure in the MA salt solutions was the same as described above. We note that exposure of the glass slides to oxygen plasma was essential in order to achieve optically smooth films. After drying of the converted films in a nitrogen stream, they were covered with a poly(methyl methacrylate) (PMMA) layer to prevent degradation by ambient moisture. For this purpose, a solution of PMMA (10 mg/mL) was dissolved in 1 mL of chlorobenzene and spincoated at 1000 rpm for 45 seconds.

Characterization details: Solar simulated AM 1.5 sunlight was generated with an ABET class AAB solar simulator calibrated to give 102 $mWcm^{-2}$ using an NREL calibrated KG5 filtered silicon reference cell. The spectral mismatch factor was calculated to be 2%. The JV curves were recorded with a Keithley 2400. The active area of the solar cells was defined with a metal aperture mask of about 0.08 cm^2.

Steady-state absorption spectra were acquired with a Varian Cary 300 UV/Vis spectrophotometer using an integrating sphere. The films were measured in a one-pass configuration, so in order to account for the highly reflective nature of the metal cathode, the optical densities were doubled as a first approximation. The FTO absorption was quantified as previously,[3a] where transmittance and reflectance were measured for the glass/FTO/air system in an integrating sphere.

Field Code Changed

Incident Photon to Charge Carrier Efficiency (IPCE) spectra were obtained using a Fourier transform photocurrent spectrometer, incorporating a Fourier transform spectrometer (Vertex 80v, Bruker), current preamplifier (SR570, Stanford Research Instruments) and custom-built control electronics and software. The spectrometer was configured with a tungsten-halogen light source and CaF_2 beam splitter. Photocurrent was recorded from short-circuited devices following the application of 2 V forward bias. The spectra were calibrated against measurements taken with the same system on a reference silicon photodiode with a known IPCE spectrum. The solar cells and reference diode were masked with a metal aperture to define the active area of ~0.0625 cm^2.

Time-resolved PL measurements were acquired using a time correlated single photon counting (TCSPC) setup (FluoTime 300, PicoQuant GmbH). The samples were photoexcited using a 507 nm laser head (LDH-P-C-510, PicoQuant GmbH) pulsed at 500 kHz, with a pulse duration of 117 ps and fluence of ~300 $nJcm^{-2}$/pulse. The samples were exposed to the pulsed light source set at 3 μJcm^{-2}/pulse fluence for ~10 minutes prior to measurement to ensure stable sample emission. The PL was collected using a high resolution monochromator and hybrid photomultiplier detector assembly (PMA Hybrid 40, PicoQuant GmbH).

Scanning electron microscopy (SEM) images were obtained using a Hitachi S-4300 microscope.

Energy dispersive X-ray (EDX) spectra were acquired with an EDAX Si(Li) detector. The spectrum shown in Figure S4 was acquired over 32 min at a dwell time of 102.4 µs and 5 eV/channel.

EEL spectra were recorded with a post column filter (Gatan Tridiem 863 P) at a dispersion of 0.2 eV in diffraction mode (camera length 102 mm).

Supporting Information
Supporting Information is available from the Wiley Online Library or from the author.

Acknowledgements
† These authors contributed equally to the work. The authors acknowledge funding from the Excellence Cluster "Nanosystems Initiative Munich" (NIM), the Center for NanoScience (CeNS) and from the Bavarian Research Network "Solar Technologies Go Hybrid".

Received: ((will be filled in by the editorial staff))
Revised: ((will be filled in by the editorial staff))
Published online: ((will be filled in by the editorial staff))

((Insert Figure here. Note: Please do not combine figure and caption in a textbox or frame.))

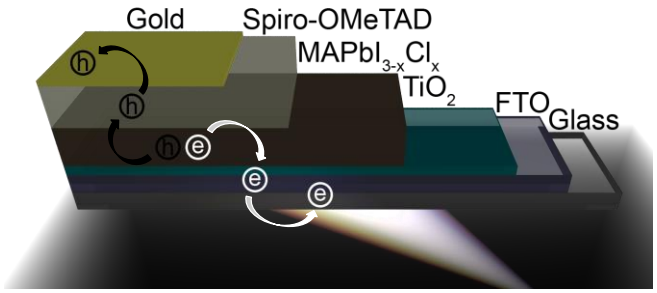

Figure 1. Schematic of the device structure. The expected charge transfer process is denoted via arrows.

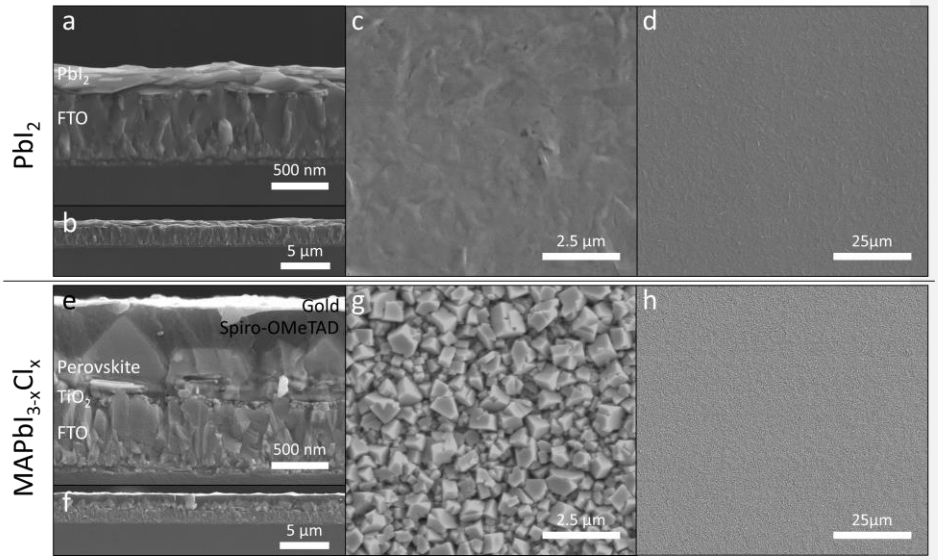

Figure 2. a) and b) SEM cross-sectional images of the as-deposited PbI_2 film on TiO_2-coated FTO. SEM top view images of the same PbI_2 films, with high magnification c) and low magnification d). e) and f) SEM cross-sectional images of the fully converted PbI_2 film (from the top row) into $MAPbI_{3-x}Cl_x$ with high magnification g) and low magnification h). All layers are labeled in the image.

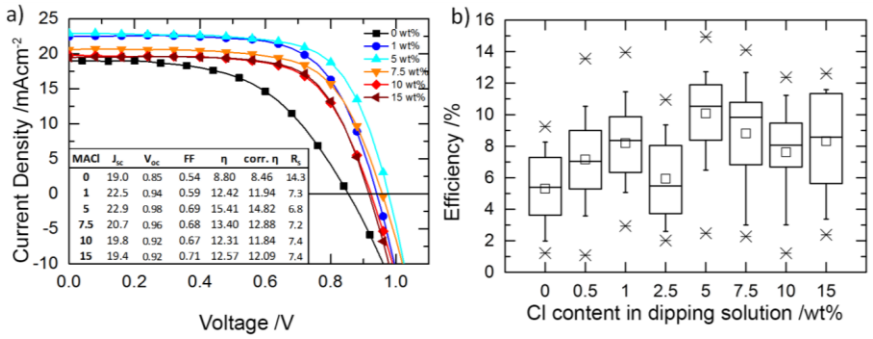

Figure 3. a) JV curves measured under AM 1.5 solar irradiance and 104 mWcm^{-2} equivalent light intensity conditions for the best performing MA lead halide perovskite devices for a range of MACl concentrations in the immersion solution. The inset summarizes the photovoltaic parameters: short circuit current (J_{sc}, mA cm^{-2}), open circuit voltage (V_{oc}, V), fill factor (FF, %), power conversion efficiency (η, %), and series resistance (R_s, Ω cm^2). A spectral mismatch factor of 1.02 was calculated for the devices prepared in this study, resulting in an equivalent 104 mWcm^{-2} irradiation intensity.[18] b) The efficiency values are shown as Box plots for efficiency distributions for a range of MACl wt% concentrations in the immersion solution. Whiskers represent the 10/90 percentile while box edges represent the 25/75 percentile. Small square symbol inside the boxes represents the mean, while the line across the boxes represents the median. The X symbols represent the maximum and minimum values. Each box represents the statistical distribution of between 30 and 40 working devices prepared under similar conditions.

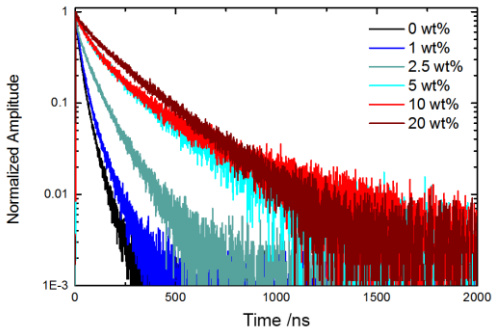

Figure 4. Time-resolved PL decay plots of MA lead mixed halide perovskite systems for a range of wt% MACl concentrations in the immersion solutions. The excitation wavelength was chosen at 507 nm, the laser head was pulsed at 500 kHz with an excitation fluence of 0.3 μJcm^{-2}/pulse, and the resulting PL was measured at 778 nm.

MACl content in solution [wt%]	Afast [A.U.]	τfast [± 1 ns]	Aslow [A.U.]	τslow [± 1 ns]
0	1205	18	3494	55
1	2900	22	932	74
2.5	1150	33	1325	112
5	919	91	401	316
10	1018	90	400	364
20	537	80	1016	262

Table 1. Summary of the biexponential fit decay parameters for the PL decays shown in Figure 4.

[1] a) A. Kojima, K. Teshima, Y. Shirai, T. Miyasaka, *JACS* **2009**, *131*, 6050-6051; b) J. H. Im, C. R. Lee, J. W. Lee, S. W. Park, N. G. Park, *Nanoscale* **2011**, *3*, 4088-4093.

[2] a) L. Etgar, P. Gao, Z. S. Xue, Q. Peng, A. K. Chandiran, B. Liu, M. K. Nazeeruddin, M. Gratzel, *JACS* **2012**, *134*, 17396-17399; b) H. S. Kim, C. R. Lee, J. H. Im, K. B. Lee, T. Moehl, A. Marchioro, S. J. Moon, R. Humphry-Baker, J. H. Yum, J. E. Moser, M. Gratzel, N. G. Park, *Sci. Rep.* **2012**, *2*; c) M. M. Lee, J. Teuscher, T. Miyasaka, T. N. Murakami, H. J. Snaith, *Science* **2012**, *338*, 643-647.

[3] a) J. M. Ball, M. M. Lee, A. Hey, H. J. Snaith, *Energy. Environ. Sci* **2013**, *6*, 1739-1743; b) A. Abate, D. J. Hollman, J. Teuscher, S. Pathak, R. Avolio, G. D'Errico, G. Vitiello, S. Fantacci, H. J. Snaith, *JACS* **2013**.

[4] P. Docampo, J. M. Ball, M. Darwich, G. E. Eperon, H. J. Snaith, *Nat. Commun.* **2013**, *4*.

[5] J. Burschka, N. Pellet, S.-J. Moon, R. Humphry-Baker, P. Gao, M. K. Nazeeruddin, M. Gratzel, *Nature* **2013**, *499*, 316-319.

[6] M. Liu, M. B. Johnston, H. J. Snaith, *Nature* **2013**, *501*, 395-398.

[7] D. Liu, T. L. Kelly, *Nat. Photon.* **2013**, *advance online publication*.

[8] a) S. D. Stranks, G. E. Eperon, G. Grancini, C. Menelaou, M. J. P. Alcocer, T. Leijtens, L. M. Herz, A. Petrozza, H. J. Snaith, *Science* **2013**, *342*, 341-344; b) G. Xing, N. Mathews, S. Sun, S. S. Lim, Y. M. Lam, M. Grätzel, S. Mhaisalkar, T. C. Sum, *Science* **2013**, *342*, 344-347.

[9] C. Wehrenfennig, G. E. Eperon, M. B. Johnston, H. J. Snaith, L. M. Herz, *Adv. Mater.* **2013**, n/a-n/a.

[10] S. Colella, E. Mosconi, P. Fedeli, A. Listorti, F. Gazza, F. Orlandi, P. Ferro, T. Besagni, A. Rizzo, G. Calestani, G. Gigli, F. De Angelis, R. Mosca, *Chem. Mater.* **2013**, *25*, 4613-4618.

[11] E. Edri, S. Kirmayer, A. Henning, S. Mukhopadhyay, K. Gartsman, Y. Rosenwaks, G. Hodes, D. Cahen, *Nano Lett.* **2014**.

[12] T. Baikie, Y. Fang, J. M. Kadro, M. Schreyer, F. Wei, S. G. Mhaisalkar, M. Graetzel, T. J. White, *J. Mater. Chem. A* **2013**, *1*, 5628-5641.

[13] S. Colella, E. Mosconi, P. Fedeli, A. Listorti, F. Gazza, F. Orlandi, P. Ferro, T. Besagni, A. Rizzo, G. Calestani, G. Gigli, F. De Angelis, R. Mosca, *Chem. Mater.* **2013**.

[14] T. Ishihara, *J. Lumin.* **1994**, *60*, 269-274.

[15] P. E. Shaw, A. Ruseckas, I. D. W. Samuel, *Adv. Mater.* **2008**, *20*, 3516-3520.

[16] P. Docampo, A. Ivaturi, R. Gunning, S. Diefenbach, J. Kirkpatrick, C. M. Palumbiny, V. Sivaram, H. Geaney, L. Schmidt-Mende, M. E. Welland, H. J. Snaith, *J. Mater. Chem. A* **2013**, *1*, 12088-12095.

[17] a) S. Sun, T. Salim, N. Mathews, M. Duchamp, C. Boothroyd, G. Xing, T. C. Sum, Y. M. Lam, *Energy. Environ. Sci* **2014**; b) J. Y. Jeng, Y. F. Chiang, M. H. Lee, S. R. Peng, T. F. Guo, P. Chen, T. C. Wen, *Adv. Mater.* **2013**.

[18] H. J. Snaith, *Energy. Environ. Sci* **2012**, *5*, 6513-6520.

Solution-deposited-converted perovskite solar cells: PbI_2 planar films were converted into the phase pure, mixed halide perovskite $(H_3CNH_3)PbI_{3-x}Cl_x$ (see picture) for the first time, exhibiting record-breaking photovoltaic performance and close to unity internal incident photon to electron conversion.

Keyword

Pablo Docampo, † Fabian Hanusch, † Samuel D. Stranks, Markus Döblinger, Johann M. Feckl Michael B. Johnston, Henry J. Snaith, Thomas Bein*

Solution Deposition-Conversion for Planar Heterojunction Mixed Halide Perovskite Solar Cells

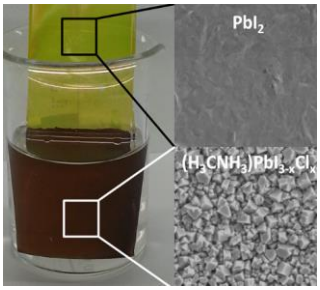

Supporting Information

Solution Deposition-Conversion for Planar Heterojunction Mixed Halide Perovskite Solar Cells

*Pablo Docampo,[†] Fabian Hanusch,[†] Samuel D. Stranks, Markus Döblinger, Johann M. Feckl Michael B. Johnston, Henry J. Snaith, Thomas Bein**

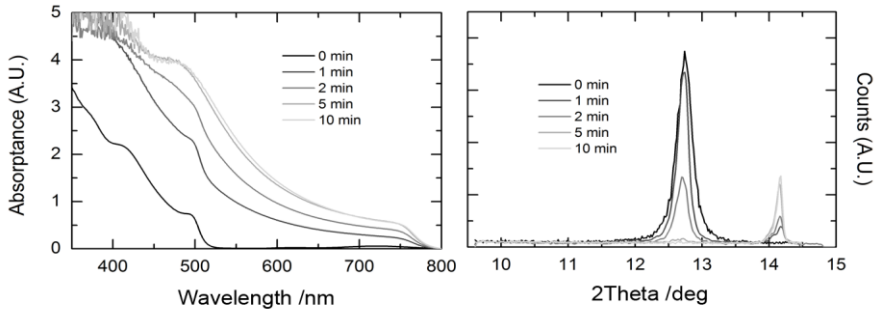

Figure S1. (Left): UV-Vis absorption spectrum of the samples immersed in a 10 $mgmL^{-1}$ MAI solution for different times. The feature at 500 nm corresponds to PbI_2, the absorption onset of the perovskite is at 760 nm. (Right): XRD of the same samples. The feature at 12.6° 2Θ corresponds to the PbI_2 (001) reflection, whereas the features at 14.2° 2 Θ corresponds to the perovskite (110) and (002) reflections.

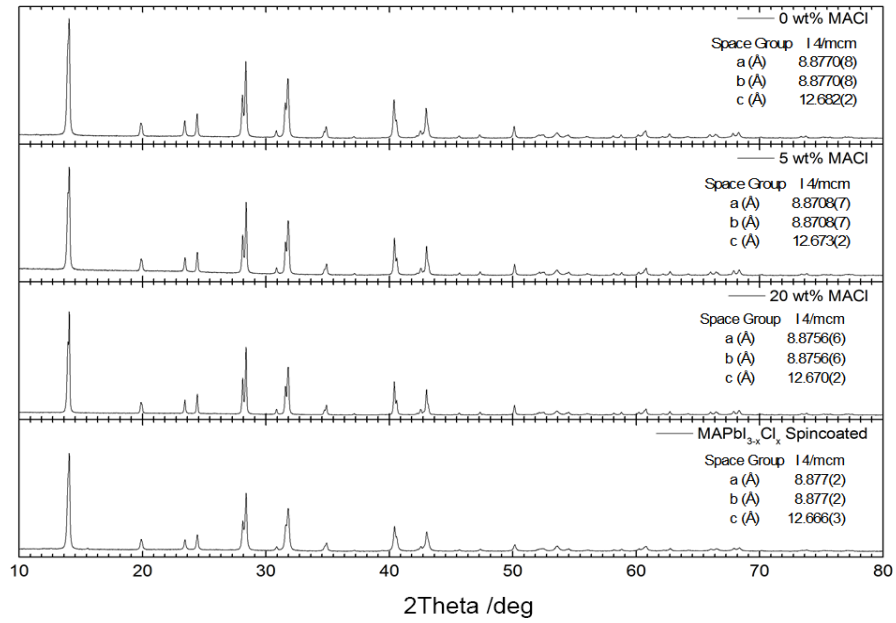

Figure S2. Wide angle X-ray diffraction patterns of samples with different Cl^--content in the immersion solution and extracted unit cell parameters.

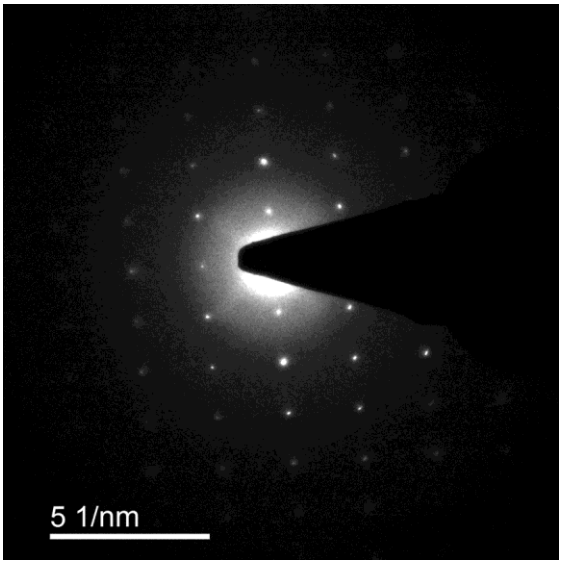

Figure S3. Electron diffraction pattern of $MAPbI_{3-x}Cl_x$. The lattice plane distances determined for the reflections closest to the primary beam in vertical and horizontal direction correspond to 0.63 nm and 0.45 nm, respectively. For a given tetragonal crystal with a=8.877

and c=12.66, as determined by powder XRD, this allows for a 0kl indexing of the reciprocal plane visible in the electron diffraction pattern. The observed reflection condition 0kl: k, l=2n supports the choice of the space group I4/mcm.

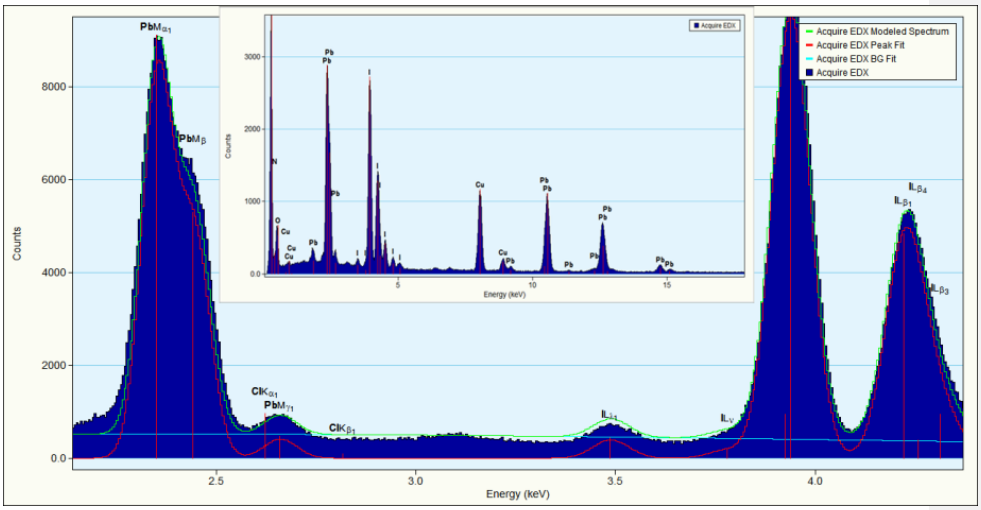

Figure S4. EDX spectrum of $MAPbI_{3-x}Cl_x$. The spectrum mainly shows Pb, I, C and Cu. The Cu-peaks and a major part of C-signal are due to the sample substrate, a carbon film coated copper grid. A possible Cl signal at 2.6 keV from Cl-Kα is overlapping with Pb Mγ1. The peak fit for the Pb-M lines does not leave any significant intensity to be attributed to the Cl-Kα line. This means that the Cl concentration is below the detection limit of the setup.

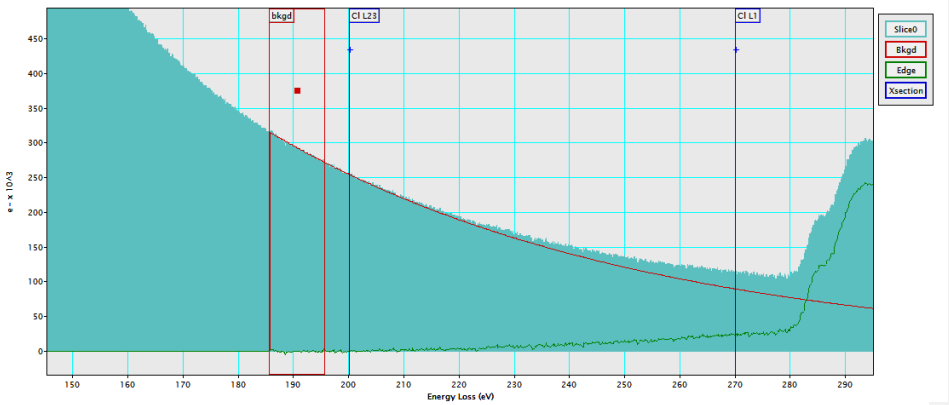

Figure S5. EEL spectrum of $MAPbI_{3-x}Cl_x$. The relevant edges typical for Cl at 200 eV loss could not be detected.

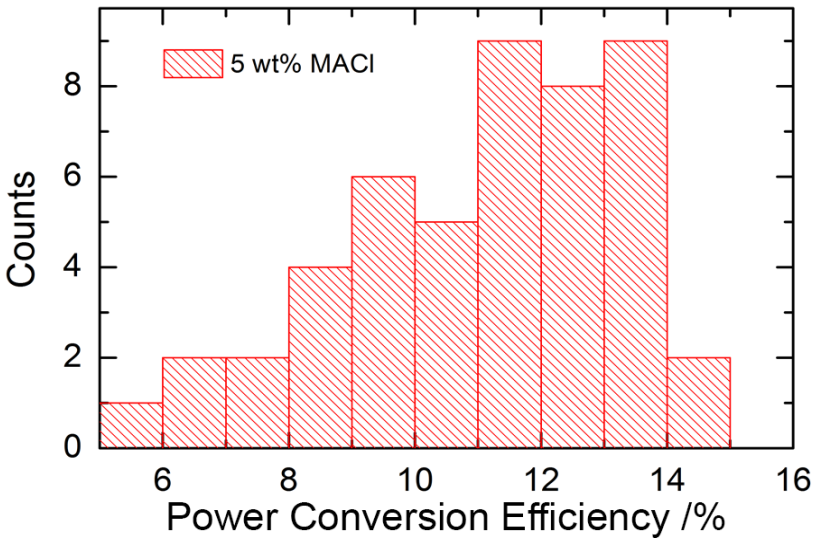

Figure S6. Power conversion efficiency histogram for a batch of 40 devices fabricated with 5 wt% MACl in the immersion solution.

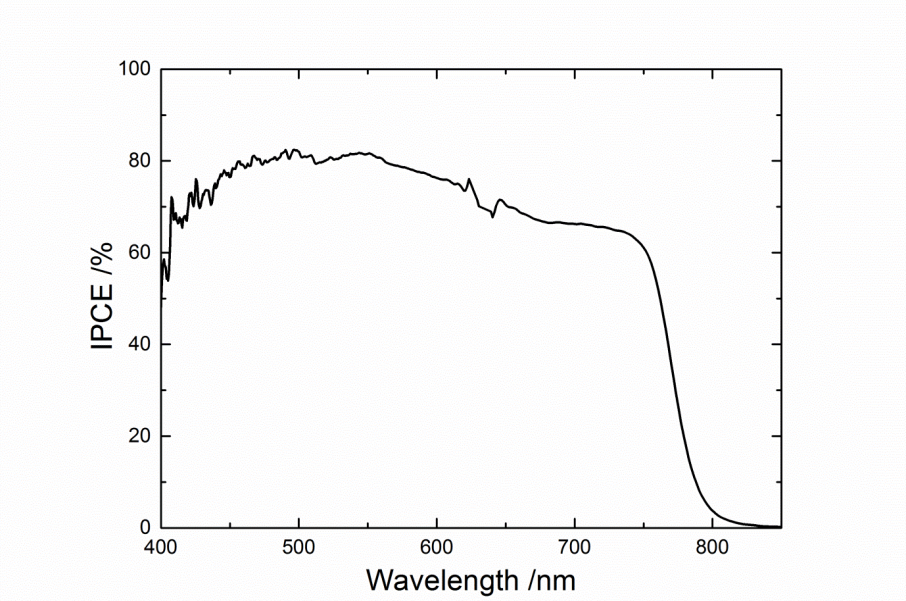

Figure S7. IPCE spectrum of the best performing device with 5 wt% MACl in the dipping solution.

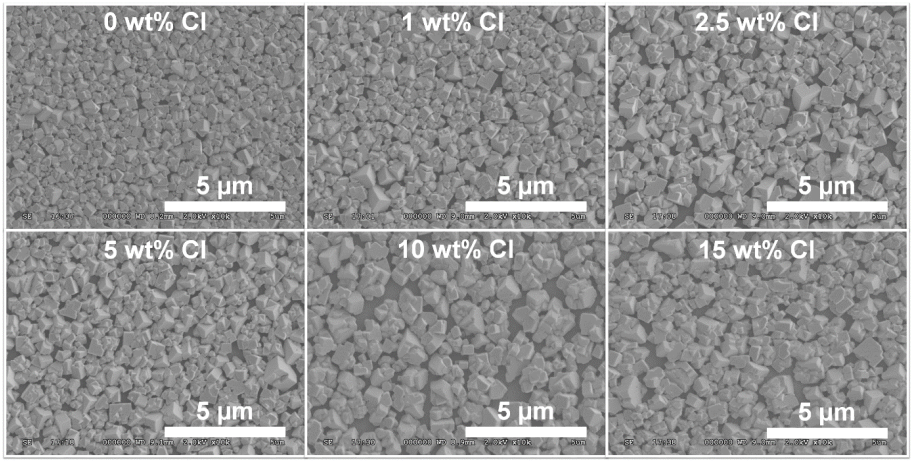

Figure S8. Top-view SEM images of perovskite films which were converted with a range of MACl concentrations in the immersion solution.

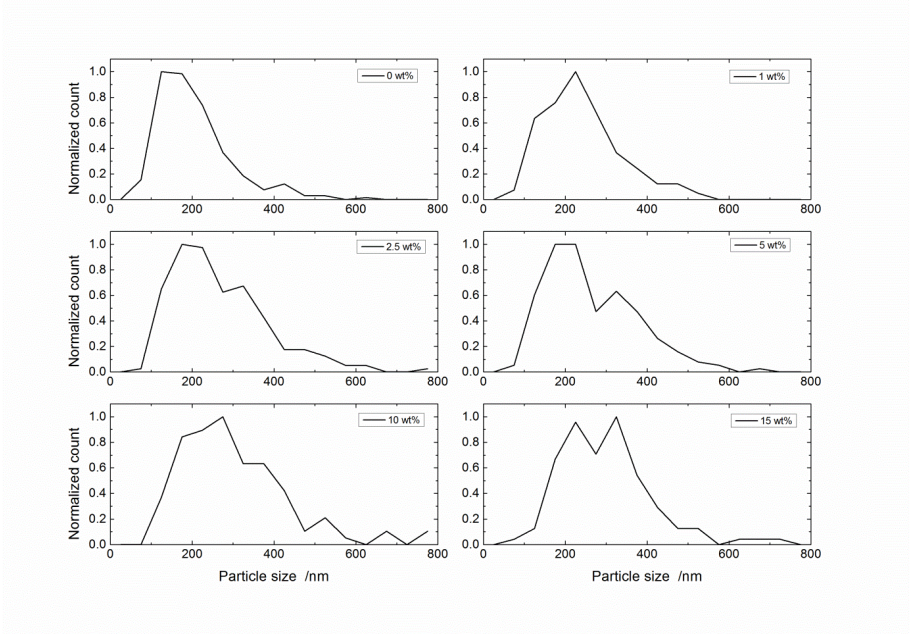

Figure S9. Particle size distribution derived from the top-view SEM images presented in Figure S8, obtained through visual analysis.

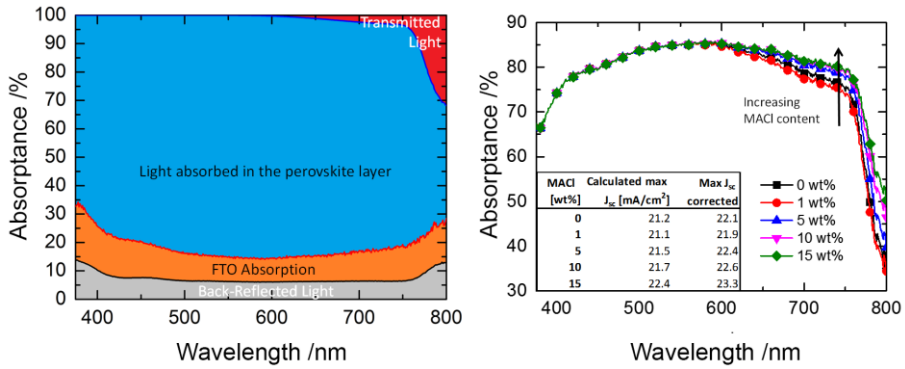

Figure S10. (Left): Spectral quantification of the light absorbed in each of the layers of the device, labelled in the figure. (Right): UV-Vis absorption spectrum of perovskite films prepared through the deposition/conversion method with different MACl concentrations in solution. All measurements were taken with an integrating sphere. The optical densities obtained were doubled as a first approximation to account for the 2 passes of light due to the presence of the highly reflective metal electrode. The maximum short circuit current (max J_{sc}) was estimated by integrating the solar spectrum with the absorptance values after subtracting the device reflectance and contributions from the FTO electrode. The values were corrected for a spectral mismatch of 1.02 and solar simulator lamp power of 102 mWcm^{-2} (denoted as max J_{sc} corrected) for direct comparison with the JV curves presented in Figure 3.

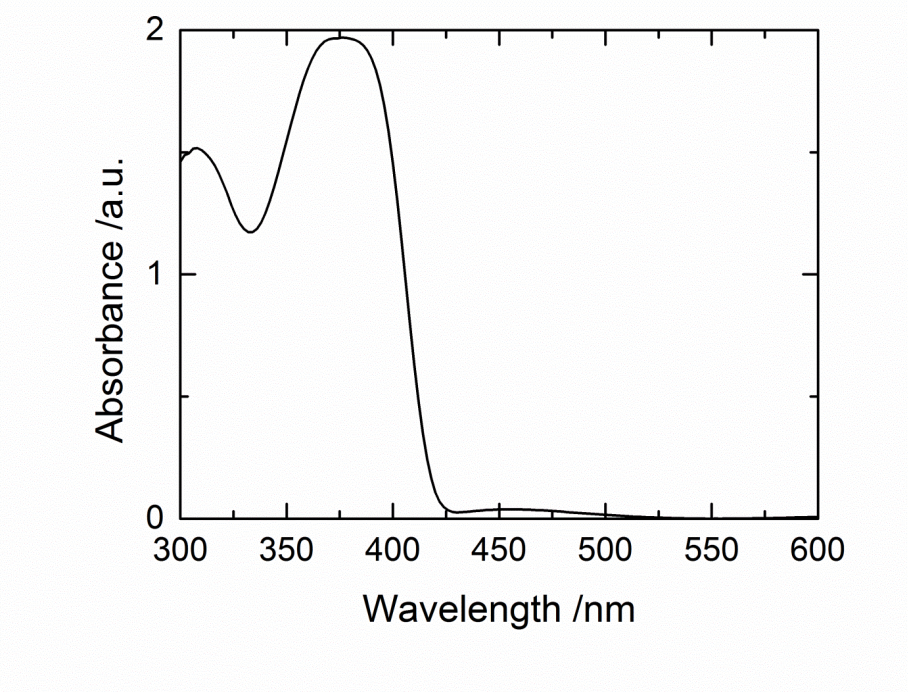

Figure S11. UV-Vis absorbance spectrum of the used spiro compound on glass.